An-Najah University Journal for Research – A
Natural Sciences

Development of a Photopolymerized Molecularly Imprinted Polymers (MIPs) Coated Surface Plasmon Resonance (SPR) Sensor for the Sensitive Determination of Sulfamethazine in Food Products

Asaad A. Sfoog[1*]

(Type: Full Article). Received: 24th Dec. 2025, Accepted: 26th Feb, 2026, Published: 1st Mar. 2026,
DOI: https://doi.org/10.35552/anujr.a.a2824

(This article belongs to the Special Issue: Sustainable Materials and Chemistry for Energy and Environmental Applications)

Abstract: This research reports the successful development of a novel optical chemosensor for the determination of sulfamethazine (SMZ) based on a surface plasmon resonance (SPR) transducer coated with a molecularly imprinted polymers (MIPs) thin film, the MIP recognition layer was fabricated directly onto a gold SPR chip via a facile and controlled in-situ photopolymerization process, using SMZ as the template, methacrylic acid as the functional monomer, and ethylene glycol dimethacrylate as the cross-linker. Characterization of the surface via a scanning electron microscope (SEM), an atomic force microscope (AFM), Fourier transform infrared (FT-IR) spectra and contact angle evaluations validated the creation of a homogeneous. The resulting SPR-MIP sensor presented excellent analytical performance, with a broad linear dynamic range from 0.1 to 50 µM and a low limit of detection (LOD) of 0.003 µM for SMZ, the sensor evinced outstanding selectivity, showing a significantly higher response to SMZ compared to structurally similar analogues such as sulfadiazine and sulfamerazine, with a high imprinting factor of 5.75. Furthermore, the sensor evinced excellent reusability and operational stability, retaining over 95% of its initial binding capacity after ten consecutive regeneration cycles, the practical applicability of the sensor was successfully validated by analyzing SMZ in spiked cow's milk samples, achieving excellent recovery rates ranging from 91.7% to 101.5%. The research specifically focuses on a robust and promising platform that combines the high selectivity of MIPs with the immediate sensitivity of SPR, offering possibilities for implementing accurate and cost-effective systems for fast and reliable food safety monitoring.

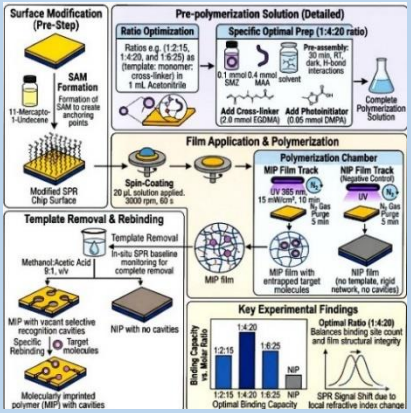

Keywords: Molecularly imprinted polymer, Photo-initiated polymerization, Surface Plasmon Resonance (SPR), Sulfamethazine, Food Safety.

Introduction

The antibiotic sulfamethazine (SMZ) is extensively used in veterinary medicine and is one of the most harmful pollutants in food. It is very hard to find its residues, especially in complex mixtures like milk, and often requires a lot of work before they can be tested [1]. Ensuring food safety necessitates the advancement of sophisticated analytical technologies that can deliver selective and dependable molecular identification in intricate sample matrices [2]. Molecularly imprinted polymers (MIPs) are innovative synthetic materials that perfectly imitate biological recognition systems. Polymerizing a three-dimensional polymer network around a target template molecule yields nano-cavities with the same form, size, and functional arrangement [3]. In the field of food analysis, MIPs have made a lot of progress. This allows faster and more reliable food additive and contaminant detection [4]. Monitoring sulfamethazine residues is a public health issue, not just an analytical difficulty. Effective monitoring systems are vital for implementing public health policies and protecting the population [5]. Recent advances in the domains of optical sensors, biosensors, tissue engineering scaffolds, and drug delivery systems demonstrate the potential of light-emitting materials with selective recognition elements for next-generation food safety analysis tools. This progress consequently opens avenues for investigating more sophisticated and sensitive optical transduction mechanisms [6, 7].

Advanced research shows that accurate material structure management is the key to producing high-performance optical devices [8]. Precision and reliability in fabrication are essential for using photonic crystals' unique optical capabilities [9]. Recently improved manufacturing processes have increased their application as biosensors, tissue engineering scaffolds, and drug delivery systems. This convergence of nanomaterial science and the biological sciences shows how precisely engineered optical structures can be used to create highly sensitive interactive interfaces with biological systems and biomolecules, proving that engineered optical platforms can detect biologically relevant molecules [10]. Thus, finding manufacturing methods that achieve optical characteristics,

1 Directore General of Education in Thi-Qar, Ministry of Education, Iraq
* Corresponding author: asaad.abdullah.qq@utq.edu.iq

mechanical strength, and simplicity of production is essential to developing genuine and meaningful sensor devices [11].

Exact engineering of the recognition element-transducer interface is foundational to the construction of high-performance sensors. Direct development of ZnO nanorods on electrodes is only one example of how research has shown the significance of nanostructural surface alteration [12]. An effective strategy to improve the accessibility of binding sites has been successfully demonstrated in the selective extraction of a related sulfonamide from water samples, and when applied to Molecularly Imprinted Polymers (MIPs), the surface imprinting approach emerges as a promising way to enhance sensor performance [13]. Comprehensive studies have shown the feasibility and reliability of using MIPs for antibiotic analysis, which is a well-established research topic [14]. Photonic Crystals (PCs) and other nano-engineered optical transduction platforms have demonstrated the capacity to detect biological molecules with high sensitivity and without the need for labels [15]. A combination of MIP technology and photonic crystals has been effectively used to detect sulfonamides [16], and other small organic molecules [17], showing how effective and flexible this method is. Additional research has shown that sulfonamides may be quickly detected using the MIP-PC platform even in complicated actual food matrices [18], with the potential to achieve outstanding selectivity, even to the point of distinguishing between chiral enantiomers [19]. There are now improvements in this area that are meant to make things easier, like naked-eye detection [20], and new science reviews have shown that it is fully grown [21]. Problems like not being able to work with watery samples must be solved before the method can be used in real life. Researchers have found hydrophilic MIPs that work well in milk and water to solve this problem [22]. Ultimately, sensor performance depends on precise chemical and physical fundamentals: the rational selection of the functional monomer to ensure strong and selective binding to the template [23], and the control over the physical architecture of the MIP layer, such as forming a thin and uniform film analogous to "core-shell" structures, to maximize binding efficiency [24].

This research, therefore, aims to design and fabricate a novel optical sensing platform that synergistically integrates the pre-programmed selectivity of a molecularly imprinted polymer, the superior label-free sensitivity of surface plasmon resonance, and the precise fabrication control afforded by photopolymerization, by developing an SPR sensor coated with a photochemically synthesized thin MIP film directly on the transducer surface, this work seeks to establish a rapid, highly sensitive, and selective analytical method for the quantitative determination of sulfamethazine in complex food matrices, thereby overcoming the principal limitations of conventional analytical techniques.

Materials and Methods

Materials and Chemical Reagents

Sulfamethazine (SMZ; $C_{12}H_{14}N_4O_2S$, M.W. 278.33 g/mol, ≥99% purity), selected as the template molecule, was purchased from Sigma-Aldrich (St. Louis, MO, USA). To rigorously evaluate the sensor's selectivity, two structurally similar analogues from the same sulfonamide family, sulfadiazine (SDZ; $C_{10}H_{10}N_4O_2S$, ≥99%) and sulfamerazine (SMR; $C_{11}H_{12}N_4O_2S$, ≥99%), were obtained from the same supplier, the primary functional monomer, methacrylic acid (MAA; 99%), was chosen for its ability to form dual hydrogen bonds with the amine and amide groups of the sulfamethazine molecule, the cross-linker, ethylene glycol dimethacrylate (EGDMA; 98%), and the Type I photoinitiator capable of photocleavage, 2,2-dimethoxy-2-phenylacetophenone (DMPA; 99%), were also purchased from Sigma-Aldrich. MAA and EGDMA were used after passing them through an alumina column to remove inhibitors, and MAA was stored at 4 °C. The surface anchoring agent, 11-mercapto-1-undecene, used to create a covalently-binding self-assembled monolayer (SAM), was procured from Sigma-Aldrich. All solvents, including acetonitrile (ACN), methanol (MeOH), ethanol (EtOH), and glacial acetic acid (AcOH), were of HPLC grade to ensure they were free of impurities. All buffer and aqueous solutions were readied using ultrapure deionization (DI) (the resistivity = 18.2 MΩ·cm) obtained from a Milli-Q water purification system (Millipore, Bedford, MA, USA). SPR sensor chips (model AU. 0001.S) coated with a 2 nm titanium adhesion layer followed by a 50 nm gold layer on a glass substrate (SF10) were purchased from Reichert Technologies (Buffalo, NY, USA).

Instrumentation and Equipment

All SPR experiments were performed using a two-channel Reichert SR7500DC Surface Plasmon Resonance system (Reichert Technologies, USA), operating in the Kretschmann configuration and utilizing a p-polarized laser diode light source with a wavelength of 780 nm, the temperature of the flow cell was precisely maintained at 25.0 ± 0.1 °C using a Peltier control system, the thin polymer films were prepared using a WS-650Mz-23NPPB Spin Coater (Laurell Technologies, USA) to ensure film thickness and homogeneity, the photopolymerization process was carried out in a sealed, nitrogen-purged chamber using a 100 W high-pressure mercury UV lamp (Oriel Instruments, USA) equipped with a narrow-band filter to select the 365 nm wavelength. Surface topography and roughness analysis of the polymer films were characterized using an Atomic Force Microscope (AFM) (Dimension Icon, Bruker, USA) operating in tapping mode with silicon probes (RTESPA-300), the surface morphology of the films was examined using a Scanning Electron Microscope (SEM), The samples were analyzed using a Nicolet iS50 FT-IR spectrophotometer, model FEI Quanta 250 (FEI, USA), at an accelerating voltage of 10 kV. To evaluate changes in surface wettability, static water contact angles were measured using a DataPhysics Instruments, Germany-based OCA 15EC Contact Angle Goniometer using the sessile drop technique and a 5 µL droplet volume.

Preparation and Modification of the SPR Chip Surface

The surface preparation process is a critical step to ensure robust and stable immobilization of the polymer layer. To begin, the gold chips were immersed for 2 minutes in a newly created "Piranha" solution, which is a 3:1 v/v combination of H_2SO_4 and 30% H_2O_2. After that, the chips were washed in ultrapure water and ethanol, and then dried under a moderate stream of high-purity nitrogen. In order to produce a self-assembled monolayer (SAM), the chips were washed and then submerged in an ethanolic solution of 11-mercapto-1-undecene with a concentration of 2 millimoles for a period of eighteen hours in a dry and dark environment. This allowed the terminal vinyl group ($-CH=CH_2$) to extend outwards and act as a covalent anchor in the subsequent polymerization reaction, while the terminal thiol group (-SH) was able to form a strong chemical bond with the gold surface. Before using the modified chips, they were rinsed with ethanol to remove adsorbed thiol molecules and then dried with nitrogen.

Photopolymerization of the Molecularly Imprinted Polymer (MIP) Layer

The pre-polymerization solution was prepared by dissolving the components at a varied molar ratio of (1:2:15, 1:4:20, and 1:6:25) as (template: monomer: cross-linker) in 1 mL of

acetonitrile. Specifically, 0.1 mmol of sulfamethazine (SMZ) was dissolved with 0.4 mmol of methacrylic acid (MAA) in the solvent. This mixture was left to pre-assemble in the dark for 30 minutes at room temperature, allowing for the formation of stable complexes between the template and functional monomer via hydrogen bonding. Afterward, 2.0 mmol of ethylene glycol dimethacrylate (EGDMA) and 0.05 mmol of the photoinitiator (DMPA) were added to the solution and mixed thoroughly; the exact composition of the polymerization solution is summarized in Table 1. A 20 µL volume of this solution was applied to the center of the chemically modified SPR chip, which was then spun at 3000 rpm for 60 seconds to form a thin, uniform liquid layer, the chip was immediately transferred to the polymerization chamber, purged with nitrogen gas for 5 minutes to remove inhibitory atmospheric oxygen, and then exposed to UV light (365 nm, intensity ~15 mW/cm²) for 10 minutes, in parallel, a non-imprinted polymer (NIP) film was readied as a negative control using the same protocol but with the omission of the sulfamethazine template from the initial formulation. The methodology illustrates the entire sensor fabrication process, from surface modification to template removal: a clean gold SPR chip, chemical modification of the surface by forming a self-assembled monolayer (SAM) of 11-mercapto-1-undecene to create anchoring points, application of the pre-polymerization solution containing the template (SMZ), monomers, and photoinitiator using the spin-coating technique, photopolymerization under UV light to form a rigid polymer network entrapping the template molecules, the template removal step to create selective, shape- and chemically-complementary nanocavities, and the selective rebinding event of SMZ molecules into the cavities, leading to a local refractive index change and thus a shift in the SPR signal. The results exhibited that MIPs with a ratio of (1:4:20) have the highest binding capacity compared to other ratios, balancing between the number of high-affinity binding sites and the structural integrity of the polymer film.

Table (1): Detailed composition of the pre-polymerization solution (1 mL) used for MIP layer preparation.

Component	Final Concentration (mM)	Volume / Weight (per 1 Ml solvent)	Role
Sulfamethazine (SMZ)	100	27.8 mg	Template
Methacrylic acid (MAA)	400	34.4 µL	Functional Monomer
EGDMA	2000	398.5 µL	Cross-linker
DMPA	50	12.8 mg	Photoinitiator

Surface Characterization and Template Removal

The prepared MIP and NIP chips underwent a series of surface analyses to confirm the success of the fabrication process. Scanning Electron Microscopy (SEM) was utilized to examine the surface morphology on a larger scale and to ensure the polymer film was free of cracks or significant defects. Atomic Force Microscopy (AFM) was used to obtain 3D topographical images and to measure the root-mean-square (Rq) roughness of the surfaces before and after the template removal process. Water contact angle measurements were performed on the bare gold, SAM-modified surface, and MIP/NIP films before and after removal, to track changes in surface energy and verify the success of each step. The template removal was performed effectively and monitored in-situ within the SPR flow cell. A regenerating wash solution consisting of methanol: acetic acid (9:1, v/v) was continuously pumped over the MIP film surface at a flow rate of 50 µL/min for 5 min (SPR baseline). The SPR signal was constantly monitored until it returned to a stable and constant baseline, confirming the complete elution of SMZ template molecules and the creation of vacant recognition cavities.

SPR Sensing Measurements and Analytical Performance Evaluation

All kinetic binding measurements were conducted at 25 °C utilizing phosphate-buffered saline (PBS, 10 mM, pH 7.4) as the running buffer. After achieving a stable baseline post-template removal, a series of sulfamethazine solutions of increasing concentrations (from 0.1 to 50 µM) were injected over both sensor channels (MIP and NIP) for 3 minutes each, followed by a 5-minute dissociation phase with PBS. The response (in angular shifts or Response Units, RU) was recorded as a function of time. A calibration curve was constructed by plotting the equilibrium response (Req) against the logarithm of the SMZ concentration, the limit of detection (LOD) was calculated using the equation (3σ/S), where σ is the standard deviation of five baseline noise measurements and S is the slope of the calibration curve, the sensor's selectivity was evaluated by injecting solutions of SDZ, SMR, and an unrelated compound at a concentration of 10 µM and comparing their responses to that of SMZ at the same concentration, the imprinting factor (IF = Response_MIP / Response_NIP) and the selectivity coefficient (α = IF_SMZ / IF_Analogue) were calculated to quantitatively assess sensor performance according to equations 1 and 2. Reusability was assessed by completing 10 consecutive cycles of binding (10 µM, SMZ) and regenerating (2-minute wash with methanol/acetic acid solution).

$$\mathrm{IF} = \frac{\mathrm{Response_{MIP}\ (RU)}}{\mathrm{Response_{NIP}\ (RU)}} \quad (1)$$

$$\alpha = \frac{\mathrm{IF_{targer}}}{\mathrm{IF_{interferent}}} \quad (2)$$

Application to Real Samples and Recovery Assessment

An analysis was performed on fresh cow's milk samples that were acquired from a nearby market in order to determine whether or not the sensor is applicable for real-world studies. To eliminate proteins and lipids that were causing interference, a straightforward sample pretreatment was carried out. 5 mL of milk was mixed with 5 mL of acetonitrile and vortexed vigorously for 1 minute; the mixture was left to stand for 15 minutes to ensure complete protein precipitation. Subsequently, the mixture was centrifuged at 10,000 rpm for 10 minutes at 4 °C, and the clear supernatant (the extract) was collected and passed through a 0.22 µm PTFE syringe filter. Recovery experiments were conducted by spiking three different concentration levels of sulfamethazine (e.g., 5, 10, and 15 µM) into the SMZ-free milk extract, these spiked samples were then analyzed using the developed SPR-MIP sensor under optimal conditions, the percentage recovery was calculated as [(Measured concentration / Spiked concentration + Original concentration) × 100%] to evaluate the sensor's accuracy and the effect of the sample matrix on its performance (equation 3).

$$\mathrm{R} = \frac{\text{Measured concentration}}{\text{Spiked concentration} + \text{Original concentration}} * 100\% \quad (3)$$

Results and Discussion

Physicochemical Characterization of the Sensor Surface

The construction of a successful SPR-MIP sensor critically depends on the controlled formation of a thin, uniform, and robustly anchored polymer layer on the gold surface; therefore, a comprehensive, multi-technique characterization was

performed at each fabrication stage to verify the surface modifications and confirm the success of the molecular imprinting process.

Surface Morphology Analysis (SEM, AFM, and FT-IR)

A scanning electron microscope (SEM) was utilized to analyze the surface morphology of the produced MIP before the washing process (before removal), MIP after the washing process (after removal), and NIP. both the MIP before the washing process (before removal) and NIP surfaces, as depicted in Figures 1(a) and (c), have a very uniform appearance and are devoid of tiny flaws like cracks, pinholes, or polymer aggregates (which seem comparatively smooth and non-porous). This exceptional homogeneity reveals that the spin-coating method at 3000 rpm evenly dispersed the pre-polymerization solution, and the photopolymerization maintained this homogeneity, creating a continuous polymer layer. After washing the template (Figure 1 (b)), the surface becomes porous and sponge-like, with cavities, unlike NIP and MIP before removal [25]. This considerable change verifies imprinting and the creation of target-molecule-specific recognition and sensing sites. To reduce noise and improve SPR signal dependability, the surface plasmon wave must interact with a constant dielectric environment over the sensing region.

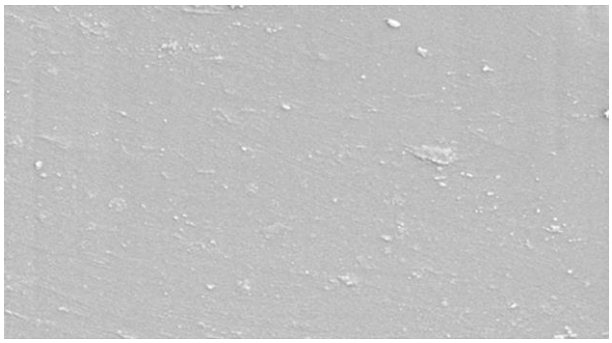

(a)

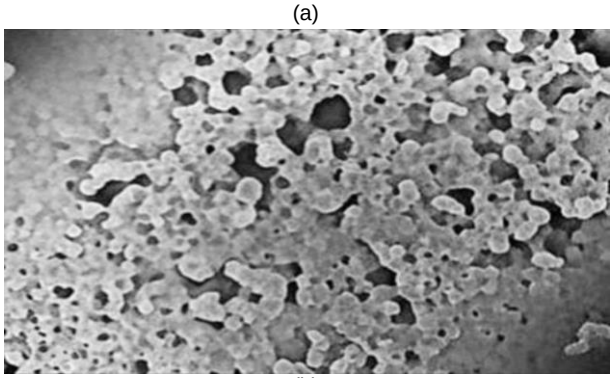

(b)

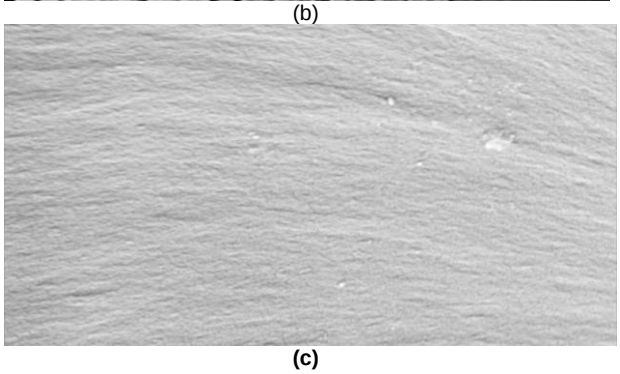

(c)

Figure (1): The SEM micrographs of (a) MIP before excessive washing, (b) MIP after excessive washing, and (c) NIP.

Atomic Force Microscopy (AFM) was utilized on the gold surface (Figure 2 (a)), MIP before washing (Figure 2 (b)), and MIP after washing (Figure 2 (c)) to better understand nanoscale topography. The 3D AFM pictures indicate the effect of imprinting and template removal. Before template removal, the MIP surface has a reasonably regular and fine granular topography (Figure 2 (b)). As evident in Figure 2 (c), the surface becomes considerably more complex and rougher, with the appearance of a nano-sponge-like structure [26]. The removal of the SMZ template molecules left a morphological "footprint" of many scattered nanocavities on the surface, indicating a successful imprinting process.

This change was quantified by measuring the root-mean-square roughness (Rq), as summarized in Table 2. The Rq value for the MIP film more than doubled, increasing from 1.7 nm to 4.1 nm after template removal. This large contrast is direct evidence that the template molecules were indeed entrapped within the polymer matrix and were successfully removed; in contrast, the NIP film showed only a minor, insignificant increase in roughness. Consequently, the porous architecture offers an increased specific surface area, facilitating a higher concentration of target molecules to adhere within the penetration depth of the evanescent field. This results in a more pronounced alteration of the local refractive index at the interface, hence enhancing the SPR signal shift [27].

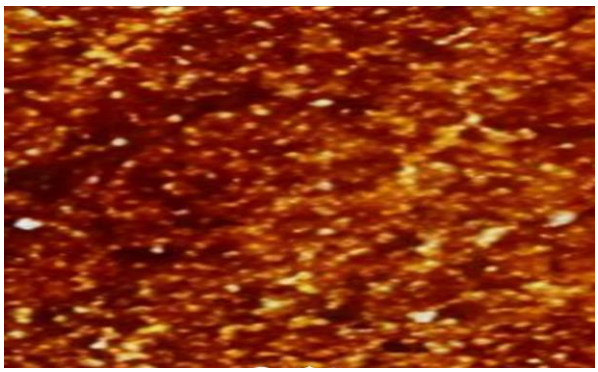

(a)

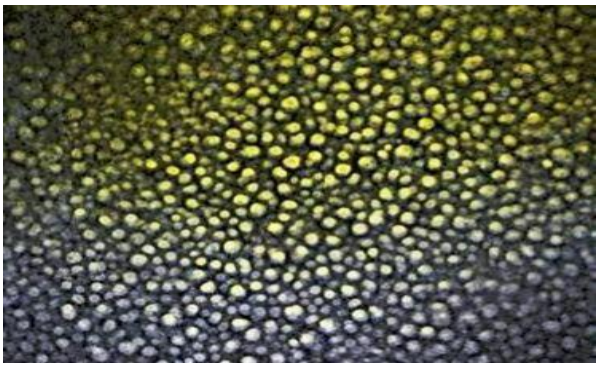

(b)

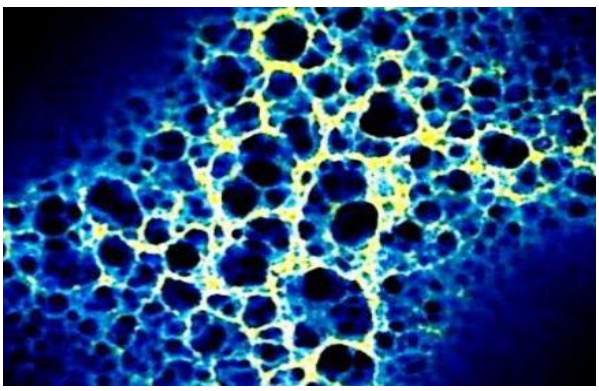

(c)

Figure (2): AFM images of (a) bare gold surface, (b) MIP before excessive washing, and (c) MIP after excessive washing.

Figure 3 demonstrates the FT-IR spectra of the prepared polymers; the spectrum of the MIP before washing shows characteristic peaks attributed to the sulfamethazine (SMZ). Sulfonamide Group (-SO2NH-) appeared at 1434 cm^{-1} of asymmetric stretching of SO2. Stretching vibrations of C=C and C=N (imine) in the pyrimidine ring at 1612–1689 cm^{-1}. Amino Groups (RNH2 and R2NH) exhibit sharp peaks that correlate to the stretching vibration of the primary amine (RNH2) at 3185–3220 cm^{-1}, while 3104–3120 cm^{-1} is related to the stretching vibration of the secondary amine (R2NH). After the excessive washing process, these peaks completely disappear from the spectrum of the MIP, which becomes nearly identical to the spectrum of the NIP. This correspondence confirms the complete and successful removal of the sulfamethazine (SMZ) from the designated binding sites of the MIP by breaking the hydrogen bonds between them.

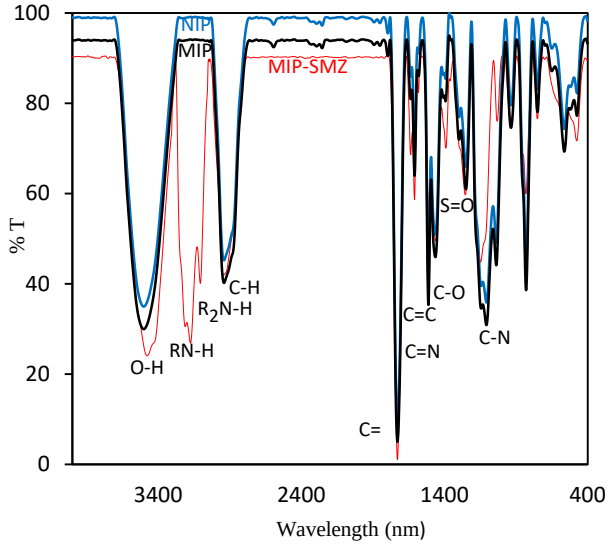

Figure (3): FT-IR spectra of (a) MIP-SMZ before excessive washing and (b) MIP after excessive washing (c) NIP.

Thermal Behavior of Polymers

Figure 4 shows the results of further characterization procedures used no the previously prepared MIPs and NIPs samples. These techniques include the TGA and DSC-DTA curves. A thermogravimetric analyzer (TGA) is utilized to ascertain the thermal stability of the polymeric samples that were created. The existence of imprinted cavities elevated the weight loss percentage of MIPs in comparison to NIPs. Nevertheless, MIPs exhibited the greatest proportion of weight decrease in comparison to NIPs. Due to the carbon structure of the imprinted polymers having cracked, they thermally decompose more quickly than the non-imprinted polymers, leading to greater weight loss [28]. Consequently, at temperatures below 150 °C, the weight loss is 1.73% for MIPs and 0.65% for NIPs. The weight loss characteristics of polymers are affected by the interaction of template molecules with functional monomers in the imprinted polymers. This influence stems from the fact that the imprinted polymers remove water molecules and remaining solvents trapped within their cavities [29]. Whereas, at temperatures between 225 and 440 degrees Celsius, the carbon (C), hydrogen (H), nitrogen (N), and oxygen (O) atoms in the polymer structure cause a loss of weight of 82.23% for MIPs and 82.84% for NIPs. The difference in residue weight between MIPs (12.28%) and NIPs (8.62%) is attributable to the potential degradation of imprinted sites caused by hydrogen bonding and π-π interactions of the functional monomer residues via thermal decomposition [30]. Weight loss often stabilizes at approximately 600°C [31].

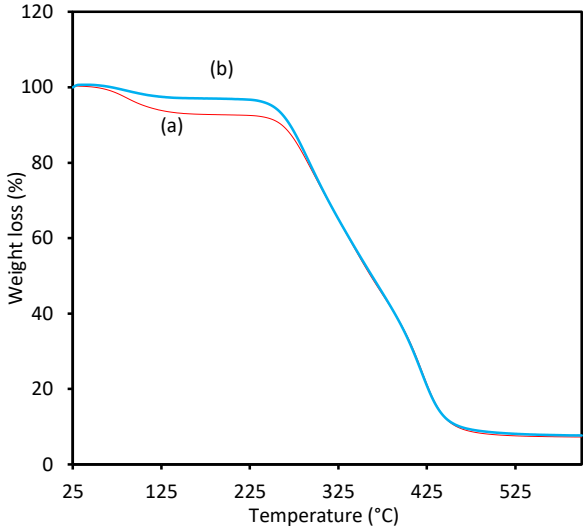

Figure (4): Thermogravimetric analysis (TGA) of: (a) MIP and (b) NIP.

The selection between differential scanning calorimetry-differential thermal analyses (DSC-DTA) is determined by the individual application and the kind of information required. DSC-DTA thermograms were applied to illustrate the difference in decomposition stages between MIP and NIP, which occurs in a single step. DSC quantifies the differential heat flow between the sample and a reference material at identical temperatures during a regulated temperature protocol, whereas DTA assesses the temperature disparity between them. DSC and DTA are both thermal analysis techniques that research the thermal behavior of materials. The weight loss manifested as an exothermic peak between 70 and 150 °C in the DSC-DTA curves of MIPs (Figure 5), whereas the DSC-DTA curves of NIPs do not exhibit this characteristic (Figure 6) [32]. The thermogravimetric curves indicated that the MIPs-based optical sensor exhibits commendable thermal stability during the imprinting processes. DSC is frequently favored for quantitative analysis (assessing energy variations), whereas DTA is more resilient and appropriate for qualitative research.

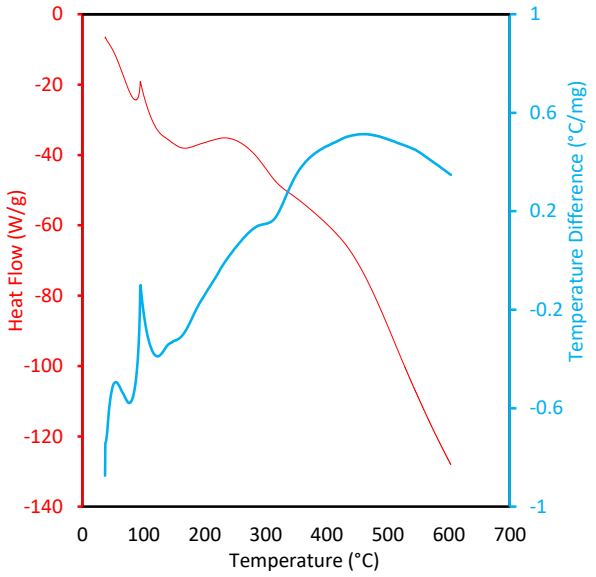

Figure (5): DSC and DTA curves of MIP.

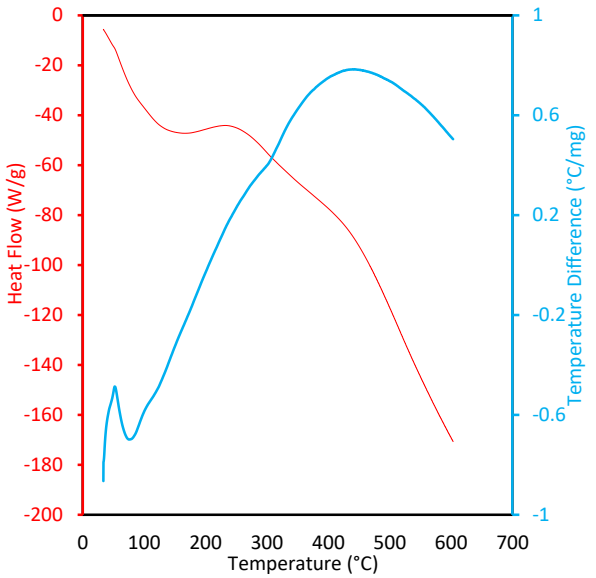

Figure (6): DSC and DTA curves of NIP.

Surface Wettability Analysis (Contact Angle)

For the purpose of detecting changes in surface chemistry, water contact angle measurements were utilized as a sensitive diagnostic methodology. As is evident seen in Table 2, every stage of the manufacturing process is associated with a fluctuation in the wetting characteristics that is anticipated; the most telling change was the significant decrease in the MIP film's contact angle to ≈ 82° after the removal of the SMZ template. This shift towards slightly increased hydrophilicity is attributed to the exposure of polar functional groups (carboxyl groups from MAA) within the cavities, which makes the surface more hydrophilic. In contrast, the NIP surface did not show this significant decrease, once again confirming the crucial role of the template in shaping the final surface architecture.

Table (2): Root-mean-square (Rq) roughness and water contact angle values for the sensor surface at different preparation stages. (Values are mean ± standard deviation of three independent measurements).

Surface	RMS Roughness (Rq) (nm)	Water Contact Angle (deg)
Clean Gold Chip	0.7 ± 0.2	66.5 ± 1.5
SAM-Modified Gold	1.1 ± 0.1	103.3 ± 1.3
MIP Film (before removal)	1.7 ± 0.2	93.1 ± 1.8
MIP Film (after removal)	4.1 ± 0.4	81.6 ± 2.0
NIP Film	2.1 ± 0.1	92.7 ± 1.6

Evaluation of the SPR Sensor Performance

After the successful fabrication of the sensor was confirmed, its analytical performance was systematically evaluated.

Binding Response and Calibration Curve

Figure 7 shows the real-time sensorgrams for the response of the MIP and NIP sensors to injections of increasing concentrations of sulfamethazine. The MIP sensor exhibited a clear, progressive increase in the SPR signal with increasing SMZ concentration, indicating an effective, concentration-dependent binding event. In contrast, the NIP sensor showed a very minimal, non-specific response, which is attributed to non-specific physical adsorption. This large difference in response is conclusive proof that the molecularly imprinted cavities are responsible for the selective and efficient binding of SMZ.

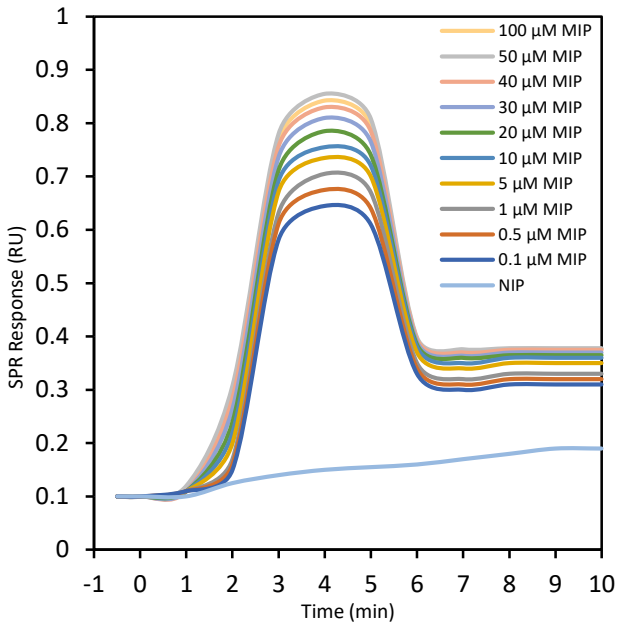

Figure (7): Real-time SPR sensorgrams showing the response of the SPR-MIP sensor for sulfamethazine detection in PBS at varying concentrations of sulfamethazine.

The results obtained in this study successfully demonstrate the development of a Molecularly Imprinted Polymer (MIP) coated Surface Plasmon Resonance (SPR) sensor for the sensitive and selective detection of sulfamethazine, the synergy between the molecular imprinting technique, the highly sensitive SPR platform, and the controlled photopolymerization process has led to the creation of a robust sensing platform with clear analytical advantages, the core of this work's success lies in the ability to fabricate a thin, homogeneous, and strongly anchored sensing layer, which was confirmed through comprehensive surface analyses. Controlling the morphological architecture of the MIP layer is critically important for achieving optimal performance, as a thin film ensures that most of the binding sites are located within the near-surface evanescent field of the surface plasmon wave, thereby maximizing the response sensitivity. This was accomplished during the formation of hydrogen bonds with the sulfamethazine (SMZ) molecule. This principle is analogous to other advanced fabrication strategies, such as the development of "core-shell" structures where a thin MIP layer is formed on nanoparticles to increase the effective surface area and improve the accessibility of the imprinted sites, as demonstrated by Ma et al, by applying spin-coating photopolymerization, we were able to achieve a similar thin "shell" architecture but on a planar substrate, ensuring maximum interaction between the analyte and the transducer [24].

Unlike some molecularly imprinted sensors that utilize hydrogel matrices which swell in water, such as the one developed by Wang et al. for the detection of imidacloprid, our sensor relies on a rigid, highly cross-linked EGDMA polymer network, while hydrogels offer excellent compatibility with aqueous environments, the rigid nature of our layer, coupled with the nanoporosity created after template removal (as confirmed by SEM and AFM measurements), offers distinct advantages, it ensures superior structural stability and prevents undesirable changes in volume or refractive index due to swelling, leading to more stable baselines and more reproducible responses, the rapid response observed in the sensorgrams indicates that diffusion within this rigid nanostructure is not a limiting factor and that the binding sites are readily accessible, thus combining the benefits of fast access and structural stability [33]. This work contributes to the broader field of molecularly imprinted optical sensors, an area that has recently seen significant progress as

reviewed by Fan et al, in the context of photonic crystal applications, whereas photonic crystals rely on structural color changes or reflection peak shifts, our platform utilizes SPR technology, which also depends on refractive index changes but offers a different transduction platform with high surface sensitivity and inherent capabilities for real-time kinetic monitoring. Our work thus expands the range of optical transduction techniques that can be successfully integrated with photochemically prepared MIP films [34].

By plotting the equilibrium response values (ΔRU) against the logarithm of the sulfamethazine concentration, the calibration curve was obtained as shown in Figure 8. The sensor demonstrated a good linear relationship in a concentration range from 0.1 to 50 µM, with a correlation coefficient (R^2) of 0.9891; the limit of detection (LOD) was calculated to be 0.003 µM. This high sensitivity makes the sensor suitable for food safety monitoring applications.

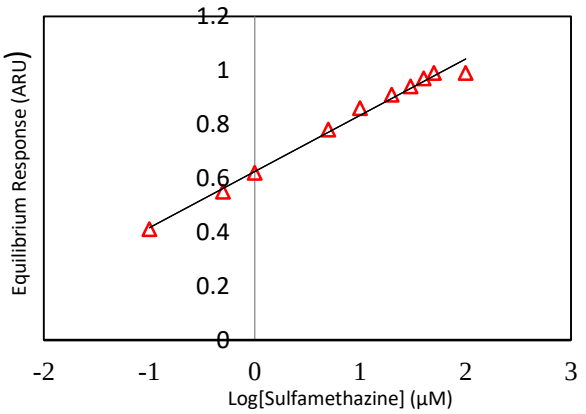

Figure (8): The calibration curve for the SPR-MIP sensor by plotting the Equilibrium response (ΔRU) against the logarithm of sulfamethazine concentrations in the range of 0.1 to 50 µM.

Subsequently, comparing our sensor's performance to existing molecular-level imprinted optical sensors, we discover that it is extremely competitive. For instance, the limit of detection (LOD) of 0.003 µM achieved in our work is in the same range as, or even better than, that reported by Çimen et al. for a molecularly imprinted photonic crystal sensor for L-phenylalanine detection. This performance similarity highlights that the SPR platform, when combined with an optimized MIP layer, can rival the sensitivity of other resonant optical platforms like photonic crystals, while offering the added advantage of commercially accessible SPR instrumentation and fluidics (LOD of 0.0085 µM) [35]. It is also important to place our work in the broader context of sulfamethazine sensors that utilize different recognition elements. For example, numerous electrochemical sensors have been developed for sulfonamide detection, such as the molecularly imprinted electrochemical sensor reported by Ayankojo et al. Our SPR-based optical approach offers a complementary alternative, providing label-free, real-time detection that allows for the study of binding kinetics (association and dissociation rates), information not easily obtained from most endpoint electrochemical measurements [36]. Likewise, Liang et al. developed an aptamer-based fluorescent sensor for sulfamethazine detection, while aptamers, like antibodies, offer excellent affinity and selectivity, our MIP-based approach offers the intrinsic advantages of synthetic receptors: superior stability in extreme temperatures and pH, long shelf-life, low production cost, and no batch-to-batch variability. This robustness makes MIP sensors more suitable for rugged field and routine applications [37]. Our MIP sensor avoids the problems of antibody production, stability, and cost, offering a potential foundation for the subsequent generation of fast screening tools; this synthetic approach also differs from electrochemical immunosensors [38], and conventional immunoassays [39]. This work exemplifies the creation of an innovative sensor, showcasing the efficacy of merging precise polymer chemistry with sophisticated optical transduction techniques to formulate resilient analytical solutions that surpass the intrinsic limitations of conventional methods and platforms reliant on biological receptors.

Selectivity

The selectivity of the sensor was evaluated by comparing its response to SMZ with its response to structurally similar analogues (SDZ and SMR) and an unrelated compound (caffeine). As shown in Figure 9, the response of the MIP sensor to SMZ was significantly higher than its response to any of the interfering compounds, proving the cavities' ability for fine discrimination.

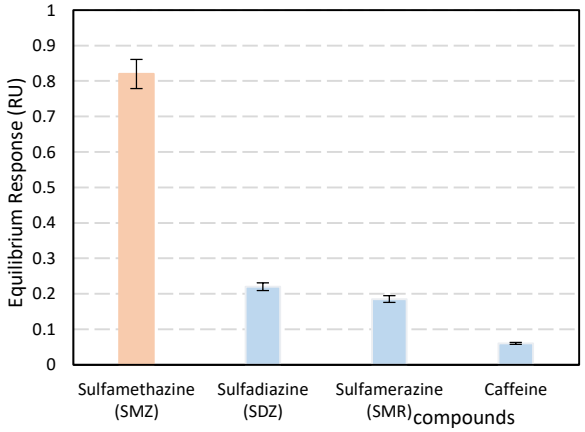

Figure (9): Response of the SPR-MIP sensor to sulfamethazine (SMZ), structurally similar analogues (SDZ, SMR), and an unrelated compound (Caffeine) at a concentration of 10 µM.

The quantitative results are summarized in Table 3. The imprinting factor (IF) for SMZ reached 5.75, while it was much lower for the other compounds. The selectivity coefficients (k) against SDZ, SMR, and caffeine were 4.13, 3.66, and 5.58, respectively, demonstrating that the sensor can effectively differentiate between sulfamethazine and other closely related sulfonamides. The determined Imprinting Factor (IF = 5.75) is markedly superior to other values documented in contemporary literature for sulfonamide detection utilizing SPR-MIP sensors [40, 41]. The elevated efficiency is ascribed to the photopolymerization technique, executed at ambient temperature. This method, in contrast to thermal polymerization, safeguards the integrity of the pre-polymerization complex and sustains robust hydrogen bonding between the sulfamethazine template and the functional monomers. As a result, this led to the formation of more precisely defined and high-affinity binding sites, as demonstrated by the elevated imprinting factor (IF) and the superior selectivity coefficient (α) against structural analogues such as sulfadiazine, sulfamerazine, and caffeine.

Table (3): Selectivity data for the SPR-MIP sensor. (Values are mean ± standard deviation, n=3)

Compound	MIP Response (RU)	NIP Response (RU)	Imprinting Factor (IF)	Selectivity Coefficient (α)
SMZ	242.4 ± 5.2	42.1 ±3.2	5.75	-
SDZ	61.1 ± 3.3	39.4 ±3.2	1.55	3.71
SMR	60.7 ± 3.1	37.1 ±2.4	1.63	3.52
Caffeine	42.3 ± 2.2	36.8 ±2.1	1.14	5.04

The exceptional selectivity demonstrated by the sensor, which is the most outstanding feature of this study, can be explained at the molecular level. Methacrylic acid (MAA) is thought to establish bifurcated hydrogen-bonded complexes with the amine and amide groups of the sulfamethazine molecule

during the pre-assembly phase. The capacity to accurately differentiate sulfamethazine from its closely related analogues, sulfadiazine and sulfamerazine, arises not only from shape complementarity but also from the exact spatial configuration of functional groups within the cavities. The precise spatial configuration of these hydrogen bonds becomes "imprinted" into the polymer matrix, forming a binding site that is complementary not only to the size and shape of SMZ but also to its specific electronic distribution, which other analogues are unable to replicate accurately [42]. Understanding the nature of these interactions, which can be modeled using theoretical approaches such as Density Functional Theory (DFT), as demonstrated by Hazhir et al. in their investigation of sulfamethazine's properties, is essential for the effective design of molecularly imprinted polymers (MIPs).

Reusability and Stability

The stability and reusability of the MIP sensor were evaluated by performing 10 consecutive cycles of binding and regeneration. As shown in Figure 10, the sensor maintained over 95% of its initial response after 10 cycles, with a relative standard deviation (RSD) of 3.5%, confirming its robustness and suitability for repeated use.

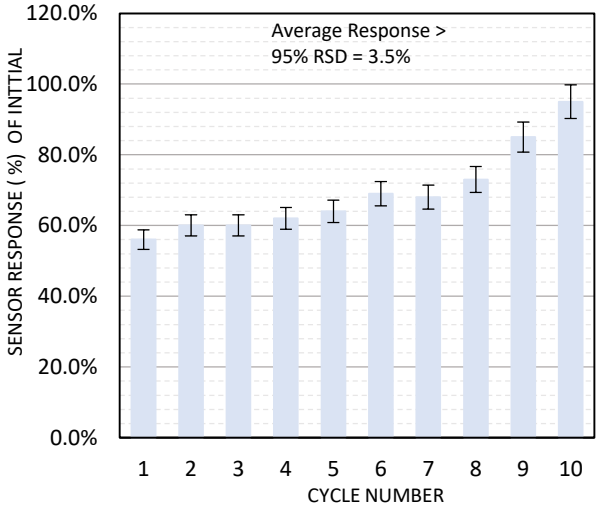

Figure (10): Evaluation of the reusability of the SPR-MIP sensor over 10 consecutive cycles of binding (10 µM of SMZ) and regeneration, the bars show the sensor response in each cycle as a percentage of the initial response.

The stability and reusability of the sensor, as demonstrated over ten consecutive cycles, are directly dependent on the robust anchoring of the polymer layer to the gold surface, while other researchers have used complex composite materials like carboxymethylcellulose/graphene oxide to enhance the dispersion and stability of MIPs, as Nie et al. did, our approach offers a simpler and more elegant solution, the use of an 11-mercapto-1-undecene SAM serves as an effective "molecular glue," where the thiol group binds the layer to the gold and the vinyl group covalently participates in the polymer network. The sensor is durable enough for practical applications since this covalent anchoring approach keeps the MIP layer fixed and does not delaminate or discharge, even after harsh washing cycles with organic solvents [43]. According to Zhao et al. in 2018, stressed that MIP-SPE materials for food applications must be compatible with aqueous samples, and the sensor's successful operation in a milk extract shows this. In spite of the EGDMA network's hydrophobic nature, the water-incompatible analyte is able to pass through the thin layer and reach the binding sites through the nanoporosity that exposes polar groups [44].

Real Sample Analysis

After undergoing an easy pretreatment, the sensor was utilized to perform an analysis of sulfamethazine in cow's milk samples. This was done in order to demonstrate the practical applicability of the sensor. An evident matrix effect was initially observed, which is the non-specific binding of milk proteins to the sensor surface [45]. An application of the sample treatment technique was made to the milk sample that contained a known concentration of sulfamethazine before the passing of the test. The preparation of a milk sample solution containing an antibiotic sulfamethazine was accomplished by adding a known concentration of sulfamethazine, and then the solution was passed through a sensor. The value of the SPR Response (RU) was disclosed. Recovery experiments were performed by spiking three known concentrations of SMZ into the milk extract according to equation 3. As shown in Table 4, the obtained recovery rates ranged from 91.7% to 101.5%, with relative standard deviations (RSDs) less than 5% (RSDs < 5%) when the original concentration was 0.3 µM. Adhering to these protocols ensures that the exceptional recovery rates observed were attributable to the Sulfamethazine concentration rather than matrix interference. These excellent results indicate that the milk matrix effect on the sensor's performance was minimal and that the developed sensor exhibits high accuracy and reliability for practical applications in food safety. Based on the results, the detection limit of this optical chemosensor for sulfamethazine was predicted to be 0.003 µM, which differs from the 8.48 nM (0.00848 µM) reported by Măgeruşan et al. (2025) when sulfamethazine was detected via an electrochemical technique based on a graphene-based sensor [46]. The reason is the discrepancy in optical techniques. Furthermore, sulfamethazine molecules are known to be photoactive. Additionally, the research conducted by Alichi et al. in 2024 found that milk samples exhibited satisfactory extraction recoveries ranging from 62 to 71%, and sensitive detection limits ranging from 0.11 ng/mL (0.000395 µM) to 0.19 ng/mL (0.000683 µM) [47]. According to the comparative performance analysis, the current study greatly outperforms the method described by Peng et al. (2024). Peng's work showed a constant adsorption rate of 64.3% over 4 cycles with a 99.7% recovery rate [41]. Our study achieves a 10-cycle operating longevity, 103% recovery, and sensor maintenance over 95%. These findings imply improved structural stability and higher analytical precision, confirming that the current sensor is more robust and efficient for the target detection in complicated matrices.

Table (4): Recovery results for the detection of sulfamethazine in spiked cow's milk samples.

Sample	Spiked Conc. (µM)	Measured Conc. (µM) (n=3)	Recovery (%)	RSD (%)
1	5.0	4.86 ± 0.12	91.7	4.3
2	10.0	10.45 ± 0.23	101.5	4.6
3	15.0	14.23 ± 0.13	93.0	4.0

Conclusions

In conclusion, this research has successfully designed, fabricated, and validated a highly sensitive and selective SPR-based sensor for the rapid, label-free determination of sulfamethazine, the innovative integration of in-situ photopolymerization for the synthesis of a MIP recognition layer directly on the SPR transducer surface proved to be a highly effective strategy, resulting in a robust sensor with excellent analytical characteristics, the developed sensor demonstrated a low limit of detection, well below the maximum residue limits set by regulatory bodies, and exceptional selectivity, enabling it to distinguish sulfamethazine from other structurally related sulfonamides, the outstanding reusability and stability, coupled

with the successful application in a complex food matrix like milk with minimal sample pretreatment, highlight the practical viability and cost-effectiveness of the proposed method. Developing the next generation of chemosensors for diverse applications requires integrating precisely engineered synthetic receptors with advanced optical transduction platforms. This research provides a very successful new food safety analysis approach and shows the integration's potential.

Disclosure statement

- **Ethics approval and consent to participate:** The Scientific Committee of the Directorate General of Education in Thi-Qar authorized this study.
- **Conflicts of interest:** The authors assert that there are no conflicts of interest pertaining to the publishing of this article.
- **Consent for publication:** Not applicable.
- **Availability of data and materials:** The raw data necessary to replicate these findings are accessible inside the text and figures of this manuscript.
- **Funding:** No external support was awarded.
- **Acknowledgements:** The author expresses gratitude to everybody who contributed to the completion of this work.

Open Access

References

1] Wang S, Wang Z, Zhang L, Xu Y, Xiong J, Zhang H, et al. Adsorption and convenient ELISA detection of sulfamethazine in milk based on MOFs pretreatment. Food Chemistry. 2022 Apr;374:131712. https://doi.org/10.1016/j.foodchem.2021.131712

2] He J, Wu M, Wang X, Xu R, Zhang S, Zhao X. Development of Molecularly Imprinted Photonic Crystals Sensor for High-Sensitivity, Rapid Detection of Sulfamethazine in Food Samples. Polymers. 2025 Jan 10;17(2):160. https://doi.org/10.3390/polym17020160

3] Mesha Mbisana, Dikabo Mogopodi, Kabomo MT, Inonge Chibua, Bonang B. M. Nkoane. Application of Molecularly Imprinted Polymers as Separation Tools for Determination of Aflatoxins in Food. Journal of Food Science. 2025 May 1;90(5). https://doi.org/10.1111/1750-3841.70259

4] Basak S, Venkatram R, Singhal RS. Recent advances in the application of molecularly imprinted polymers (MIPs) in food analysis. Food Control. 2022 Sep;139:109074. https://doi.org/10.1016/j.foodcont.2022.109074

5] Yang Y, Zhang H, Zhou G, Zhang S, Chen J, Deng X, et al. Risk Assessment of Veterinary Drug Residues in Pork on the Market in the People's Republic of China. Journal of Food Protection. 2022 May 1;85(5):815–27. https://doi.org/10.4315/JFP-21-411

6] Zhang Z, Zhang H, Tian D, Phan A, Maral Seididamyeh, Mazen Alanazi, et al. Luminescent sensors for residual antibiotics detection in food: Recent advances and perspectives. Coordination Chemistry Reviews. 2024 Jan 1;498:215455–5. https://doi.org/10.1016/j.ccr.2023.215455

7] Asif IM, Tiziano Di Giulio, Gagliani F, Cosimino Malitesta, Mazzotta E. Advances in the Direct Nanoscale Integration of Molecularly Imprinted Polymers (MIPs) with Transducers for the Development of High-Performance Nanosensors. Biosensors. 2025 Aug 6;15(8):509–9. https://doi.org/10.3390/bios15080509

8] Chen H, Wei J, Pan F, Yuan T, Fang Y, Wang Q. Advances in Photonic Crystal Research for Structural Color. Advanced Materials Technologies. 2024 Aug 3;10(4). https://doi.org/10.1002/admt.202400865

9] Zhang W, Hu Y, Feng P, Li Z, Zhang H, Zhang B, et al. Structural Color Colloidal Photonic Crystals for Biomedical Applications. Advanced Science. 2024 Jul 31. https://doi.org/10.1002/advs.202403173

10] Fathi F, Monirinasab H, Ranjbary F, Nejati-Koshki K. Inverse opal photonic crystals: Recent advances in fabrication methods and biological applications. Journal of Drug Delivery Science and Technology. 2022 Jun;72:103377. https://doi.org/10.1016/j.jddst.2022.103377

11] Zhou J, Li H, Ye L, Liu J, Wang J, Zhao T, et al. Facile Fabrication of Tough SiC Inverse Opal Photonic Crystals. The Journal of Physical Chemistry C. 2010 Dec 2;114(50):22303–8. https://doi.org/10.1021/jp108928q

12] Hatamie A, Echresh A, Zargar B, Nur O, Willander M. Fabrication and characterization of highly-ordered Zinc Oxide nanorods on gold/glass electrode, and its application as a voltammetric sensor. Electrochimica Acta. 2015 Aug;174:1261–7. https://doi.org/10.1016/j.electacta.2015.06.083

13] Sun M, Tian Y, Xu P, Du X, Weng J, He J, et al. Application of surface-imprinted polymers in pretreatment for detection of sulfamonomethoxine in water samples. Microchemical Journal. 2024 May;200:110333. https://doi.org/10.1016/j.microc.2024.110333

14] Zhao G, Zhang Y, Sun D, Yan S, Wen Y, Wang Y, et al. Recent Advances in Molecularly Imprinted Polymers for Antibiotic Analysis. Molecules. 2023 Jan 1;28(1):335–5. https://doi.org/10.3390/molecules28010335

15] Resende S, Frasco MF, Sales MGF. A biomimetic photonic crystal sensor for label-free detection of urinary venous thromboembolism biomarker. Sensors and Actuators B: Chemical. 2020 Jun 1;312:127947. https://doi.org/10.1016/j.snb.2020.127947

16] Zhang S, Shao K, Hong C, Chen S, Lin Z, Huang Z, et al. Fluorimetric identification of sulfonamides by carbon dots embedded photonic crystal molecularly imprinted sensor array. Food Chemistry. 2023 May 1;407:135045–5. https://doi.org/10.1016/j.foodchem.2022.135045

17] Liu Y, Gu H, He J, Cui A, Wu X, Lai J, et al. Rapid Screening of Butyl Paraben Additive in Toner Sample by Molecularly Imprinted Photonic Crystal. Chemosensors. 2021 Nov 6;9(11):314. https://doi.org/10.3390/chemosensors9110314

18] Li L, Lin Z, Huang Z, Peng A. Rapid detection of sulfaguanidine in fish by using a photonic crystal molecularly imprinted polymer. Food Chemistry. 2019 May;281:57–62. https://doi.org/10.1016/j.foodchem.2018.12.073

19] Zhang Y, Pan Z, Yuan Y, Sun Z, Ma J, Huang G, et al. Molecularly imprinted photonic crystals for the direct label-free distinguishing of l-proline and d-proline. Physical Chemistry Chemical Physics. 2013;15(40):17250. https://doi.org/10.1039/c3cp52213j

20] Hong X, Bai J, Peng Y, Zhang X, Gao Z, Ning B, et al. Au-doped photonic crystal allows naked-eye determination of small organic molecules. Sensors and Actuators B: Chemical. 2020 Oct;321:128493. https://doi.org/10.1016/j.snb.2020.128493

21] Li L, Li J, Xu J, Liu Z. Recent advances of polymeric photonic crystals in molecular recognition. Dyes and Pigments. 2022 Sep;205:110544. https://doi.org/10.1016/j.dyepig.2022.110544

22] Ma Y, Pan G, Zhang Y, Guo X, Zhang H. Narrowly Dispersed Hydrophilic Molecularly Imprinted Polymer Nanoparticles for Efficient Molecular Recognition in Real Aqueous Samples Including River Water, Milk, and Bovine Serum. Angewandte Chemie International Edition. 2012 Dec 17;52(5):1511–4. https://doi.org/10.1002/anie.201206514

23] Boukadida M, Anene A, Jaoued-Grayaa N, Chevalier Y, Hbaieb S. Choice of the functional monomer of molecularly imprinted polymers: Does it rely on strong acid-base or hydrogen bonding interactions? Colloid and Interface Science Communications. 2022 Sep 1;50:100669. https://doi.org/10.1016/j.colcom.2022.100669

24] Ma J, Yuan L, Ding M, Wang S, Ren F, Zhang J, et al. The study of core–shell molecularly imprinted polymers of 17β-estradiol on the surface of silica nanoparticles. Biosensors and Bioelectronics. 2010 Nov 1;26(5):2791–5. https://doi.org/10.1016/j.bios.2010.10.045

25] Awokoya KN, Oninla VO, Eugene-Osoikhia TT, Umukoro EH, Babalola JO, Fakola EG, et al. Design of ligand-based imprinted polymers for dyes sequestration from aqueous solution: Experimental and computational studies. Water Science. 2025 Oct 22;39(1):53–65. https://doi.org/10.1080/23570008.2025.2574771

26] Kaur R, Rana S, Mehra P, Kaur K. Surface-Initiated Reversible Addition–Fragmentation Chain Transfer Polymerization (SI-RAFT) to Produce Molecularly Imprinted Polymers on Graphene Oxide for Electrochemical Sensing of Methylparathion. ACS Applied Materials & Interfaces. 2024 Sep 9;16(37):49889–901. https://doi.org/10.1021/acsami.4c08168

27] Suriyanarayanan S, Olsson GD, Nicholls IA. On-Surface Synthesis of Porosity-Controlled Molecularly Imprinted Polymeric Receptors for the Biotinyl Moiety. ACS Applied Polymer Materials. 2024 Jan 8;6(2):1470–82. https://doi.org/10.1021/acsapm.3c02655

28] Murugan K, Jothi VK, Rajaram A, Natarajan A. Novel Metal-Free Fluorescent Sensor Based on Molecularly Imprinted Polymer N-CDs@MIP for Highly Selective Detection of TNP. ACS Omega. 2021 Dec 28;7(1):1368–79. https://doi.org/10.1021/acsomega.1c05985

29] Khulu S, Ncube S, Kgame T, Mavhunga E, Chimuka L. Synthesis, characterization and application of a molecularly imprinted polymer as an adsorbent for solid-phase extraction of selected pharmaceuticals from water samples. Polymer Bulletin. 2021 Feb 3. https://doi.org/10.1007/s00289-021-03553-9

30] Shah SAH, Asman S. Evaluation of deep eutectic solvent as a new monomer for molecularly imprinted polymers for removal of bisphenol A. Journal of Polymer Research. 2023 May 12;30(6). https://doi.org/10.1007/s10965-023-03581-1

31] Chen J, Huang X, Wang L, Ma C, Wu S, Wang H. The synthesis of a dual-template surface molecularly imprinted polymer based on silica gel and its application in the removal of pesticides from tea polyphenols. Analytical Methods. 2020 Jan 1;12(7):996–1004. https://doi.org/10.1039/C9AY02708D

32] Menczel JD, Andre R, Krongauz VV, Shibata K, Szécsényi KM, Grebowicz J. Handbook of Differential Scanning Calorimetry: Techniques, Instrumentation, Inorganic, Organic and Pharmaceutical Substances. Butterworth-Heinemann. 2023; 793–40. https://doi.org/10.1016/B978-0-12-811347-9.00008-4

33] Wang X, Mu Z, Liu R, Pu Y, Yin L. Molecular imprinted photonic crystal hydrogels for the rapid and label-free detection of imidacloprid. Food Chemistry. 2013 Dec;141(4):3947–53. https://doi.org/10.1016/j.foodchem.2013.06.024

34] Fan J, Qiu L, Qiao Y, Xue M, Dong X. Recent Advances in Sensing Applications of Molecularly Imprinted Photonic Crystals. 2021 Jun 14;9. https://doi.org/10.3389/fchem.2021.665119

35] Çimen D, Bereli N, Denizli A. Surface Plasmon Resonance Based on Molecularly Imprinted Polymeric Film for l-Phenylalanine Detection. Biosensors. 2021 Jan 15;11(1):21. https://doi.org/10.3390/bios11010021

36] Akinrinade George Ayankojo, Jekaterina Reut, Öpik A, Vitali Syritski. Sulfamethizole-imprinted polymer on screen-printed electrodes: Towards the design of a portable environmental sensor. Sensors and Actuators B Chemical. 2020 Jul 14;320:128600–0. https://doi.org/10.1016/j.snb.2020.128600

37] Liang N, Shi B, Hu X, Li W, Huang X, Li Z, et al. A ternary heterostructure aptasensor based on metal-organic framework and polydopamine nanoparticles for fluorescent detection of sulfamethazine. Food Chemistry. 2024 Dec;460:140570. https://doi.org/10.1016/j.foodchem.2024.140570

38] Liu X, Wen Y, Hu W, Lu X, Chen L, Zhao L, et al. A signal-amplified electrochemical immunosensor for the detection of sulfadimidine in crayfish using COOH-MWCNTs-Fe3O4-GO nanohybrids modified working electrode. Journal of Food Composition and Analysis. 2024 Oct;134:106501. https://doi.org/10.1016/j.jfca.2024.106501

39] Wang Z, Xing K, Ding N, Wang S, Zhang G, Lai W. Lateral flow immunoassay based on dual spectral-overlapped fluorescence quenching of polydopamine nanospheres for sensitive detection of sulfamethazine. Journal of Hazardous Materials. 2022 Feb;423:127204. https://doi.org/10.1016/j.jhazmat.2021.127204

40] Jiang G, Liu L, Wan Y, Li J, Pi F. Surface-enhanced Raman scattering based determination on sulfamethazine using molecularly imprinted polymers decorated with silver nanoparticles. Microchimica Acta. 2023 Apr 4;190(5). https://doi.org/10.1007/s00604-023-05744-9

41] Peng W, Huang W, Gao M, Yang W, Xu W. Novel photoresponsive molecularly imprinted polymers based on etched silicon core with enabling enhanced selectivity and sensitivity for the detection of sulfamethazine. Polymer International. 2024 Mar 25;73(7):556–62. https://doi.org/10.1002/pi.6628

42] Hazhir N, Kiani F, Tahermansouri H, Azade SGH, Koohyar F. Prediction of Thermodynamic and Structural Properties of Sulfamerazine and Sulfamethazine in Water Using DFT and ab Initio Methods. Journal of the Mexican Chemical Society. 2018 May 21;62(1). https://doi.org/10.29356/jmcs.v62i1.575

43] Nie F, Li C, Ahmad N, Yuan Z, Tan Y, Xu Y, et al. Molecularly Imprinted Polymer Based on Carboxymethylcellulose/Graphene Oxide Composites for Selective Adsorption of Hydroxycamptothecin. ACS Applied Polymer Materials. 2022 Nov 3;4(12):9294–304. https://doi.org/10.1021/acsapm.2c01549

44] Zhao X, Wang J, Wang J, Wang S. Development of water-compatible molecularly imprinted solid-phase extraction coupled with high performance liquid chromatography–tandem mass spectrometry for the detection of six sulfonamides in animal-derived foods. Journal of Chromatography A. 2018 Nov;1574:9–17. https://doi.org/10.1016/j.chroma.2018.08.044

45] Talebi Vandishi Z, Dodangeh M, Zarean Mousaabadi K. Detection of Antibiotics in Milk Using Immunosensors. Ensuring Wellness: Immunosensors Monitoring Food Quality and Pathogenicity Risks. 2025;133–57. https://doi.org/10.1007/978-3-031-97477-9_9

46] Măgeruşan L, Pogăcean F, Pruneanu S. Graphene produced via electrochemical exfoliation in instant coffee as effective sensing material for trace detection of sulfamethazine in milk samples. Microchemical Journal. 2025 Jul;214:113999. https://doi.org/10.1016/j.microc.2025.113999

47] Alichi M, Movassaghghazani M, Afshar Mogaddam MR. Dispersive solid phase extraction of some sulfonamide antibiotics from milk combined with dispersive liquid-liquid microextraction. Journal of Food Composition and Analysis. 2024 Nov;135:106631. https://doi.org/10.1016/j.jfca.2024.106631